ELSEVIER

Thermochimica Acta 326 (1999) 43–52

thermochimica acta

Synthesis, characterization and the thermal decomposition of lithium tris(oxalato)lanthanum(III)nonahydrate and sodium tris(oxalato)lanthanum(III)octahydrate

N. Deb[a,*], S.D. Baruah[b], N.N. Dass[c]

[a] *Department of Chemistry, North Eastern Regional Institute of Science and Technology, Nirjuli 791109, Arunachal Pradesh, India*
[b] *Regional Research Laboratory, Jorhat 785006, Assam, India*
[c] *Department of Chemistry, Dibrugarh University, Dibrugarh 786004, Assam, India*

Received 20 May 1998; received in revised form 30 September 1998; accepted 1 October 1998

Abstract

Lithium *tris*(oxalato)lanthanum(III)nonahydrate ($Li_3[La(III)(C_2O_4)_3{\cdot}9H_2O$(LOL)), and sodium *tris*(oxalato)lanthanum(III)octahydrate ($Na_3[La(III)(C_2O_4)_3]{\cdot}8H_2O$ (SOL)), have been synthesized and characterized by elemental analysis, IR spectral, and X-ray powder diffraction studies. Thermal studies (TG, DTG and DTA) in air showed that LOL becomes anhydrous around 198°C, followed by decomposition to Li_2CO_3, La_2O_3 and $LiLaO_2$ at ca. 542°C, via the formation of several intermediates. Finally, around 950°C, the oxide and peroxide of lithium and a trace of La_2C_3 along with La_2O_3 and $LiLaO_2$ are detected. A DSC study in nitrogen suggested the presence of lithium oxalate and La_2O_3 around 660°C. The compound, SOL, lost all eight water molecules within 230°C, followed by decomposition to Na_2CO_3 and $La_2O(CO_3)_2$ at ca. 538°C. The pyrolyzed product at 950°C contained Na_2CO_3 (trace), Na_2O, Na_2O_2 (trace), La_2O_3, probably also $NaLaO_x$. The residual product in nitrogen at 630°C is assumed to be a mixture of Na_2CO_3, NaO_2 and La_2O_3. The kinetic parameters of dehydration and decomposition have been calculated from TG curves using four non-mechanistic equations. Kinetic parameters E^*, ΔH, ΔS obtained from DSC study are discussed. Some of the decomposition products were identified by IR and X-ray powder diffraction studies. The tentative mechanism for the decomposition in air are proposed.

Keywords: Thermal decomposition; TG-DTA; Oxalato; Activation energy; X-ray powder diffraction

1. Introduction

From the viewpoint of wide applicability [1] of ferrites, the alkali iron carboxylates, mainly oxalates have been studied [2–4]. These are used as inorganic precursors for the preparation of ferrites. Some authors [5,6] have studied the iron precursors due to sensitive oxidation states and complexing ability of iron and keeping in view the formation of alkali ferrites as end-product. Thermolysis of alkali tris(oxalato/malonato)ferrates(III) have been studied [7,8], where the decomposition mode in both the precursors, $M_3[Fe(C_2O_4)_3]{\cdot}xH_2O$ and $M_3[Fe(CH_2C_2O_4)_3]{\cdot}xH_2O$ (where, M=Li, Na, K), are similar. Just like iron, the corresponding potassium oxalato metallates(III) of the type, $K_3[M(C_2O_4)_3]{\cdot}xH_2O$ (where M=Al, V, Cr, Mn, Co, Rh) had been studied [9]. Bivalent metal

*Corresponding author. Tel.: +91-360-257659; fax: +91-360-244307; e-mail: chem@nerist.ernet.in

0040-6031/99/$ – see front matter
PII: S0040-6031(98)00553-X

complexes of the type, $K_2[M(OX)_2]$ were formed [10,11] as intermediates from the compounds, $K_3[M(OX)_3]$ (where M=Mn, Co) in a nitrogen atmosphere. Although some thermal studies on *bis* and *tris*(oxalato/malonato) metallates of alkali metals have been done, the analogue with lanthanum as metal has not yet been carried out. Keeping in mind the possibility of formation of alkali-metal lanthanites and their possible applicability, we report here the synthesis, characterization and thermal decomposition of lithium *tris*(oxalato)lanthanum(III)nonahydrate ($Li_3[La(III)(C_2O_4)_3]\cdot 9H_2O$), and sodium *tris*(oxalato)-lanthanum(III) octahydrate ($Na_3[La(III)(C_2O_4)_3]\cdot 8H_2O$) in air and nitrogen. Kinetic parameters of the dehydration and decomposition steps are evaluated and probable mechanisms of decomposition are also proposed.

2. Experimental

All the chemicals used were of AR grade purity. We extended our preparative method adopted for bimetallic bivalent compounds of oxalate [12,13]. Lanthanum nitrate was converted to chloride by digesting repeatedly with concentrated hydrochloric acid. The chloride-free hydroxide was then prepared. It was dissolved in glacial acetic acid and heated on a steam bath. Then a solution of lithium chloride and sodium chloride were added separately in two portions followed by dropwise addition of a saturated solution of oxalic acid. White compounds were separated in each case and washed several times with distilled water and dried over calcium chloride. Water contents were determined gravimetrically [14] and thermogravimetrically. The metal contents were estimated by the methods available in literature. Microanalytical data were recorded with a Carlo Erba 1108 elemental analyzer.

IR spectra (200–4000 cm^{-1}) were recorded on a Perkin–Elmer IR 883 spectrophotometer. TG, DTG and DTA were carried out at 10°C min^{-1} in static air with a Shimadzu DT-30B thermal analyzer. DSC studies were performed in nitrogen using a Perkin–Elmer PC series DSC-7 at a heating rate of 10°C min^{-1}. Powder X-ray diffraction (XRD) patterns were obtained using a Rigaku X-ray diffractometer system, D/Max. IIIC.

3. Results and discussion

3.1. Characterization of complexes

The white powder compounds, $Li_3[La(III)(C_2O_4)_3]\cdot 9H_2O$ (LOL), and $Na_3[La(III)(C_2O_4)_3]\cdot 8H_2O$ (SOL) are insoluble in water and common organic solvents. However, they decompose in the presence of strong acid or alkali. The estimated metal contents, elemental and water analysis suggests the proposed formula of the compounds. The chelating nature of oxalato groups are concluded [12–16] from the IR spectra (Table 1).

3.2. Decomposition of the complexes

The TG profile (Fig. 1) of $Li_3[La(III)(C_2O_4)_3]\cdot 9H_2O$ (LOL), shows a break at 97°C, indicating the removal of the first molecule of water. At 198°C, a 24% mass loss indicates the elimination of the remaining seven molecules of water. The change in DTG between 30° and 245°C, and an endothermic peak in

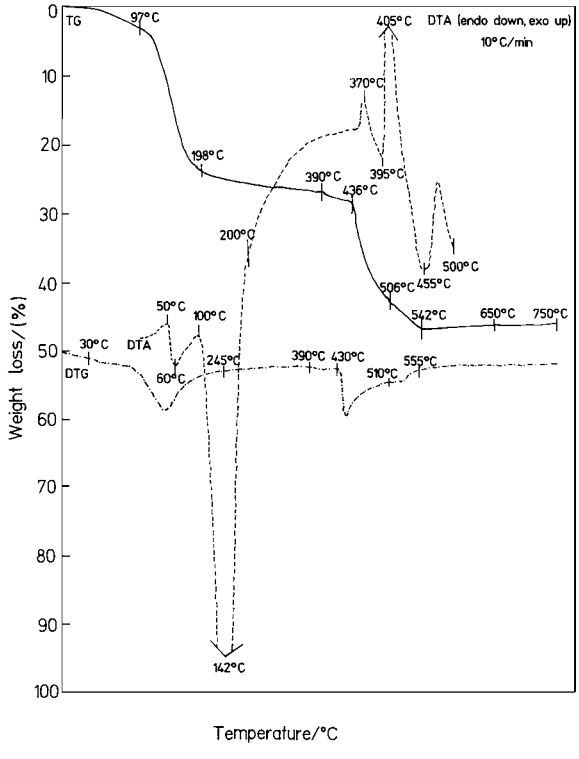

Fig. 1. TG, DTG and DTA curves of $Li_3[La(III)(C_2O_4)_3]\cdot 9H_2O$ (LOL) in air.

Table 1
Selected bands in the IR spectra of $Li_3[La(III)(C_2O_4)_3]\cdot 9H_2O$ (LOL) and $Na_3[La(III)(C_2O_4)_3]\cdot 8H_2O$ (SOL)

IR bands/cm^{-1}		Assignments
LOL	SOL	
2800–3800 [a]	3000–3760 [a]	ν_{sy}(O–H)+ν_{asy}(O–H), or hydrogen bonding
1620 [b]	1620 [b]	δ_{sy}(H–O–H)
1440–1800 [a]	1490–1800 [a]	ν_{asy}(C=O)
1370 [d,b]	1365 [d,b]	ν_{sy}(C–O) and/or ν(C–C)
1320 [b]	1325 [d,b]	ν_{sy}(C–O) and/or δ(O–C=O)
800 [b]	800 [b]	ν(La–O) and/or δ(O–C=O) or coordinated water
610 [c]	610 [c]	Water of crystallization
530 [c]	—	ν_{sy}(C–C) and/or ring deformation
460 [d], 400 [c]	460 [d], 405 [c]	ν(La–O) and/or ring deformation
354 [d]	360 [d]	δ(O–C=O)
290 [e]	308 [e]	out-of-plane bending

[a] Broad.
[b] Strong.
[c] Small.
[d] Medium.
[e] Very small.

Table 2
Kinetic data evaluated by the methods (a) Freeman and Carroll, (b) Flynn and Wall, (c) Coats and Redfern, and (d) MacCallum–Tanner equation

Compound	Step	Method	E^*/(kJ mol^{-1})	Order of reaction	A/s^{-1}	Reaction
LOL	1	a	29.40	0.4		
		b	27.80	0.5		
		c	27.60		2.10×10^2	dehydration
		d	27.30		10.60×10^6	
	2	a	63.10	0.6		
		b	59.70	1.0		
		c	61.60		3.00×10^2	decomposition
		d	62.30		13.60×10^8	
SOL	1	a	21.70	0.4		
		b	20.20	1.0		
		c	22.60		3.10×10^2	dehydration
		d	23.00		4.60×10^8	
	2	a	53.20	0.3		
		b	48.80	1.0		
		c	50.20		8.60×10^2	decomposition
		d	52.50		1.40×10^9	
	3	a	7.60	0.4		
		b	7.20	1.0		
		c	8.20		32.60	decomposition
		d	8.70		6.40×10^4	

DTA between 50° and 100°C (ΔT_{min}=60°C) followed by another large endotherm in the 100–200°C range (ΔT_{min}=142°C) correspond to the dehydration step. The activation energies (E^*) (Table 2) of this step, calculated from the TG curve using the methods of Freeman and Carroll [17], Flynn and Wall [18], Coats and Redfern [19], and the MacCallum-Tanner equations [20] are found to be in good agreement with each

other. The complete anhydrous compound appears to be formed at 390°C, which indicates the presence of coordination of water with the lanthanum atom. However, a 26.8% mass loss at 390°C indicates some rearrangement of the anhydrous form during the removal of the last trace of water. The rearranged form may be assumed [8] as an intimate mixture of $1/2Li_2C_2O_4$ and $1/2Li_6La_2(C_2O_4)_5$ (calculated loss, 26.48%) with reduction of the lanthanum atom. The reduced form is further assumed to be a mixture of $Li_2[La(C_2O_4)_2]$ and $1/2Li_2C_2O_4$. Although this type of change of state in an intermediate was reported [3,4,10,11] in the case of alkali *tris*(oxalato)metallates, we do not anticipate the same in our study in air medium. Instead, a mixture of $1/2Li_2C_2O_4$ and $Li_2[La(III)(C_2O_4)_{2.5}]$ (calculated mass loss, 27.67%) with partial rupture of $C_2O_4^{2-}$ group can be assumed. Further, a distinct step in the TG profile in the 390–436°C range with 28% mass loss suggests the constituents in the mixture are $Li_2C_2O_4$ and $Li[La(III)(C_2O_4)_2]$ (calculated mass loss, 27.67%). The exothermic peak at 370°C in DTA and a DTG change between 390 and 430°C correspond to these changes. The white pyrolysed product at 390°C with 30.12% mass loss

Table 3
X-ray powder diffraction (XRD) data of $Li_3[La(III)(C_2O_4)_3]\cdot 9H_2O$ (LOL), and pyrolysed products at 390°, 550° and 950°C in air

LOL		Pyrolysed product of LOL at 390°C		Pyrolysed product of LOL at 550°C		Pyrolysed product of LOL at 950°C [a]	
d/(Å)	I(REL)	d/(Å)	I(REL)	d/(Å)	I(REL)	d/(Å)	d/(Å)
2.15	100	7.63	88	8.47	67	2.155	1.083
2.07	73	7.26	88	6.86	75	2.063	1.069
1.99	73	6.71	97	5.61	84	2.015	1.061
1.93	58	6.06	98	5.43	84	1.965	1.053
1.89	59	5.26	100	5.11	86	1.893	1.046
1.84	54	4.87	98	4.43	100	1.824	1.037
1.78	49	4.21	73	4.17	80	1.776	1.026
1.73	45	3.87	64	3.81	66	1.715	1.018
1.69	43	3.41	52	3.59	55	1.652	1.011
1.65	43	3.30	46	3.26	85	1.594	0.998
1.60	40	3.06	37	3.06	52	1.573	0.990
1.53	42	2.84	32	2.83	29	1.540	0.980
1.51	41	2.64	31	2.64	29	1.501	0.962
1.47	36	2.57	30	2.33	29	1.474	0.947
1.44	30	2.55	32	2.28	31	1.461	0.939
1.40	36	2.49	32	2.13	23	1.436	0.925
1.36	29	2.42	26	2.08	19	1.411	0.916
1.32	29	2.38	24	2.01	15	1.396	0.909
1.30	33	2.28	26	1.92	16	1.351	0.900
1.27	27	2.25	22	1.87	21	1.325	0.890
1.25	29	2.15	23	1.81	17	1.294	0.886
1.23	27	2.09	22	1.75	18	1.273	0.878
1.21	29	2.05	23	1.69	11	1.258	0.867
1.18	24	1.97	18	1.66	13	1.240	0.855
1.17	26	1.94	19	1.65	13	1.224	0.848
1.16	26	1.86	16	1.62	11	1.213	0.839
1.14	23	1.82	14	1.56	12	1.181	0.836
1.13	26	1.74	14			1.165	0.833
1.12	26	1.69	12			1.151	0.828
1.11	27	1.63	11			1.133	0.823
		1.61	11				
		1.57	10				

[a] Relative intensities, I(REL), are not given, because scanning was done, separately at two different ranges of 2θ; one from 40–90° and the second from 90–140°.

was isolated. Its IR spectrum shows the presence of coordinated oxalato groups. The bands at ca. 1640 (very strong) and ca. 1345 cm^{-1} [8,21] substantiate the presence of $Li_2C_2O_4$ in the mixture. Some of the bands are found to be displaced in comparison with the precursor, which is due to rearrangement. However, the bands at 350, 460, 800 and 1320 cm^{-1} are similar in position to those of the precursor and indicate the coordination of $C_2O_4^{2-}$ in $Li[La(III)(C_2O_4)_2]$. The XRD data (Table 3) further confirm [22] the presence of lithium oxalate in the mixture. The remaining mismatched *d*-values may be due to $Li[La(C_2O_4)_2]$. Subsequently, in the DTA profile, an exotherm between 395 and 455°C (ΔT_{max}=405°C) is due to oxidative decomposition, followed by another medium exotherm (455–500°C) and indicates that both the compounds in the mixture decompose via the formation of an unstable intermediate. The TG curve shows a continuous mass loss from 436° to 542°C (46.5% at 542°C), which suggests the formation of $LiLaO_2$ and $2Li_2CO_3$ (calculated mass loss, 44.42%). The XRD pattern (Table 3) of the grey coloured pyrolysed product at 550°C confirmed [22] the presence of $LiLaO_2$ and Li_2CO_3. A trace of La_2O_3 is also detected from the *d*-values. Moreover, the sharp bands in the IR spectrum at 495(S), 740(w), 865(s), ca. 1450(S), ca. 1520(S) cm^{-1} further substantiate the presence of Li_2CO_3 [23,24]. The additional bands at 360(mS), 480(s) and 880(s) cm^{-1} may be due to $LiLaO_2$ and a small band at 720 cm^{-1} is due to La_2O_3 [24]. Two overlapping changes in DTG between 430° and 510°C and 510 and 555°C suggest the existence of an intermediate prior to the formation of the product at 542°C. The TG profile at 506°C, corresponding to a 43% mass loss, indicates the intermediate which is probably mixture of $Li_2C_2O_4$, Li_2CO_3 and $1/2La_2O_3$ (calculated mass loss, 42.19%). The mixture formed at 542°C slowly gains 0.5% mass and is stable in the 650–750°C range. As the DTA was recorded up to 500°C and TG up to 750°C, the possible changes in the thermoanalytical curves due to further decomposition of carbonate to oxide and probable solid–solid interaction of both the oxides could not be observed. However, the fraction of Li_2CO_3 reacts with La_2O_3, forming $LiLaO_2$ [26,27] below 540°C in TG as confirmed from X-ray studies; residual Li_2CO_3 exists up to 740°C in the presence of $LiLaO_2$. Although Li_2CO_3 melts at 720°C [25], the presence of lanthanites and oxides enhanced the stability of carbonate in the present case. Although the TG has been recorded up to 750°C, the pyrolysed product at 950°C when subjected to XRD study (Table 3) confirmed [22] the presence of La_2O_3, Li_2O (trace), Li_2O_2, $LiLaO_2$ and a trace of La_2C_3. Carbon monoxide formed during decomposition disproportionates to CO_2(g) and carbon which, in turn, gets converted to carbides of lanthanum at higher temperatures. The E^* value for the major decomposition step as calculated (Table 2) using four different methods [17–20] are found to be in good agreement. In the DSC profile (Fig. 2), an endothermic peak between 93.46° and 205.46°C is for dehydration. The reaction order is unity. Further, a flat endotherm (414.42–468.85°C) followed by a slightly larger endotherm (500–598.09°C) indicate that two intermediates are formed, either with some rearrangement or due to rupture of $C_2O_4^{2-}$ of anhydrous moiety. Finally, a sharp endotherm in a narrow (649.56–655.95°C) range is observed. The mass loss of 53.73%, after scanning up to 670°C, indicates that the end-product is a mixture of $Li_2C_2O_4$ and $1/2La_2O_3$ (calculated mass loss, 54.81%). The kinetic parameters for all the steps are evaluated through integration of the peaks and are given in Table 5.

The water vapour, carbon monoxide and carbon dioxide evolved during decomposition were confirmed by IR spectroscopy [16].

The foregoing study suggests the following tentative mechanism of thermal decomposition in air:

$$Li_3[La(C_2O_4)_3]\cdot 9H_2O \overset{\text{ca. } 97^\circ C}{\rightarrow} Li_3[La(C_2O_4)_3]$$

$$\cdot 8H_2O(s) + H_2O(v) \overset{97-198^\circ C}{\rightarrow} Li_3[La(C_2O_4)_3]H_2O(s)$$

$$+ 7H_2O(v) \overset{198-390^\circ C}{\rightarrow} 1/2Li_2C_2O_4(s)$$

$$+ Li_2[La(C_2O_4)_{2.5}](s) + H_2O(v) \overset{390-436^\circ C}{\rightarrow} Li_2C_2O_4(s)$$

$$+ Li[La(C_2O_4)_2](s) \overset{\text{ca. } 506^\circ C}{\rightarrow} Li_2C_2O_4(s) + Li_2CO_3(s)$$

$$+ 1/2La_2O_3(s) + mCO(g) + nCO_2(g)$$

$$\overset{\text{ca. } 542^\circ C}{\rightarrow} 2Li_2CO_3(s) + La_2O_3(s)(\text{trace}) + LiLaO_2(s)$$

$$+ xCO(g) + yCO_2(g) \overset{950^\circ C}{\rightarrow} LiLaO_2(s) + Li_2O_2(s)$$

$$+ Li_2O(s)(\text{trace}) + La_2O_3(s) + La_2C_3(s) + 1CO(g)$$

$$+ pCO_2(g)$$

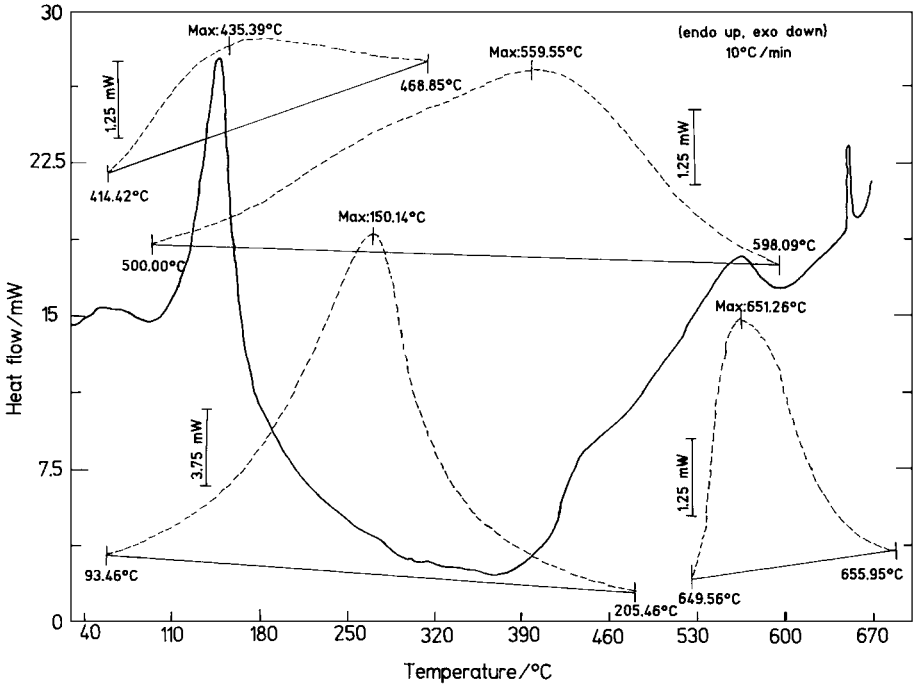

Fig. 2. DSC curves of $Li_3[La(III)(C_2O_4)_3]\cdot 9H_2O$ (LOL) in nitrogen.

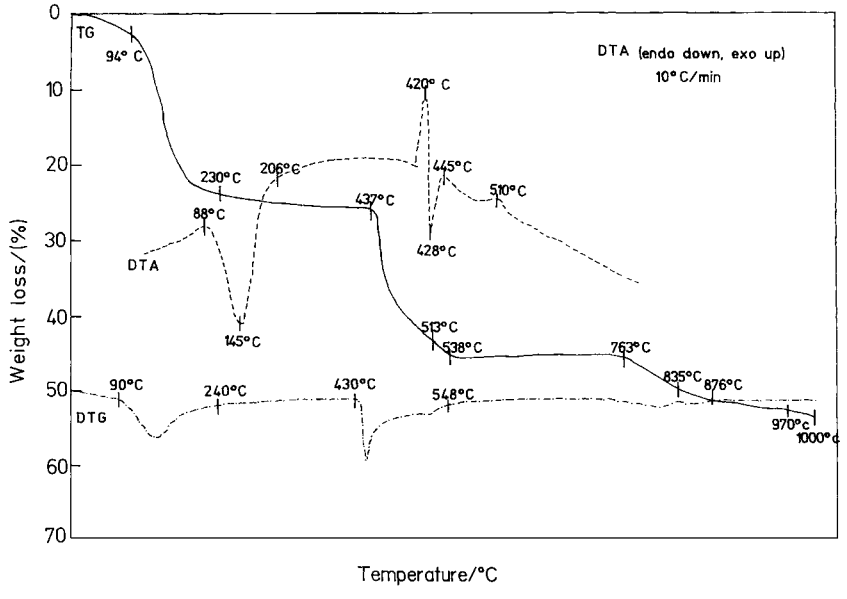

Fig. 3. TG, DTG and DTA curves of $Na_3[La(III)(C_2O_4)_3]\cdot 8H_2O$ (SOL) in air.

Table 4
X-ray powder diffraction data of $Na_3[La(III)(C_2O_4)_3]\cdot 8H_2O$ (SOL), and pyrolysed products at 280°, 550° and 950°C in air

SOL		Pyrolysed product of SOL at 280°C		Pyrolysed product of SOL at 550°C[a]		Pyrolysed product of SOL at 950°C [a]	
d/(Å)	I(REL)	d/(Å)	I(REL)	d/(Å)	d/(Å)	d/(Å)	d/(Å)
2.211	100	2.210	100	6.291	1.386	2.155	1.053
2.156	89	2.154	89	5.666	1.360	2.071	1.037
2.079	90	2.110	92	5.179	1.320	1.984	1.032
1.994	79	2.034	81	4.423	1.298	1.899	1.023
1.851	59	1.961	74	3.770	1.274	1.833	1.015
1.811	55	1.913	77	3.759	1.254	1.784	1.003
1.784	56	1.844	68	3.303	1.237	1.724	0.994
1.751	52	1.810	62	3.136	1.215	1.681	0.978
1.705	48	1.725	62	2.847	1.198	1.635	0.974
1.667	47	1.705	61	2.588	1.181	1.598	0.967
1.647	48	1.621	53	2.469	1.158	1.548	0.959
1.615	47	1.573	49	2.392	1.136	1.505	0.949
1.589	50	1.532	47	2.332	1.117	1.478	0.935
1.545	44	1.498	46	2.148	1.100	1.439	0.931
1.528	44	1.477	40	2.054	1.093	1.408	0.922
1.479	41	1.445	41	1.986	1.077	1.394	0.916
1.454	39	1.417	46	1.869	1.064	1.368	0.906
1.437	38	1.389	37	1.812	1.045	1.349	0.899
1.414	35	1.367	39	1.761	1.035	1.322	0.888
1.389	31	1.346	35	1.695	1.024	1.291	0.882
1.367	33	1.321	41	1.663	1.013	1.237	0.873
1.347	36	1.299	41	1.605	1.004	1.236	0.867
1.323	33	1.273	36	1.563	0.985	1.219	0.863
1.306	32	1.258	34	1.498	0.970	1.207	0.855
1.274	31	1.246	35	1.479	0.960	1.182	0.849
1.247	34	1.224	32	1.439	0.952	1.162	0.847
1.196	30	1.196	35	1.417	0.942	1.142	0.841
1.178	29	1.176	33			1.113	0.836
1.155	29	1.151	33			1.099	0.831
1.130	26	1.130	37			1.069	0.824

[a] Relative intensities, I(REL), are not given, because scanning was done separately at two different ranges of 2θ, between 10–60°, and between 60–110° for product at 550°C, and between 40–90° and another between 90–140° for product at 950°C.

The thermoanalytical curves (TG, DTG and DTA) of $Na_3[La(III)(C_2O_4)_3]\cdot 8H_2O$ (SOL) are shown in Fig. 3. The compound eliminates a molecule of water at 94°C and becomes anhydrous at 230°C (mass loss: found, 24%; calculated, 23.39%). An endothermic peak between 88° and 206°C (ΔT_{min}=145°C) in DTA and DTG between 90° and 240°C are for deaquation. The XRD pattern (Table 4) of the pyrolysed product at 280°C suggests the anhydrous form is isomorphous with the parent compound. A few peaks are displaced due to the disappearance of possible M–OH_2 bonds and the water of crystallisation. The IR spectrum shows the presence of bands at 350, 800, 1320, 1360 and 1620(s) cm^{-1}; which indicates the retention of $C_2O_4^{2-}$ groups. The E^* (Table 2) values of this step are found to be similar to those calculated using all the four methods [17–20]. The mass loss of 26.3% occurs very slowly in TG up to 437°C, indicating an intramolecular rearrangement through partial decomposition of the oxalato group and a subsequent separation of $Na_2C_2O_4$ from $Na[La(C_2O_4)_x]$ (where $1.5<x<2$). Further, an inclined slope from 437° to 538°C with a 45.7% mass loss indicates the formation of Na_2CO_3 and $1/2La_2O(CO_3)_2$ (calculated mass loss, 44.33%). The pyrolysed product is isolated at 550°C in air subjected to IR spectral and XRD studies. The

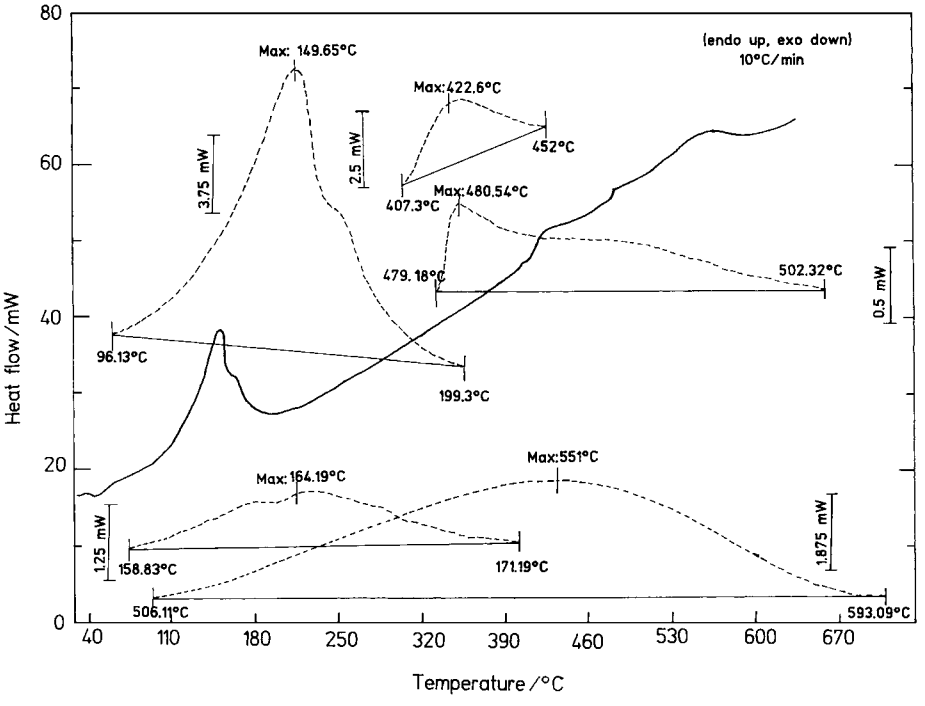

Fig. 4. DSC curves of $Na_3[La(III)(C_2O_4)_3]\cdot 8H_2O$ (SOL) in nitrogen.

Table 5
DSC data of $Li_3[La(III)(C_2O_4)_3]\cdot 9H_2O$ (LOL) and $Na_3[La(III)(C_2O_4)_3]\cdot 8H_2O$ (SOL) in nitrogen

Compound	Step	Temperature range/°C	Peak temperature/°C	ln k_0	E^*/ (kJ mol^{-1})	ΔH/ (kJ mol^{-1})	ΔS/ (J K^{-1} mol^{-1})	Order of reaction	Reaction
LOL [a]	1	93.46–205.46	150.14	23.68±0.51	99.40±2.14	297.95	704.14	1.27±0.02	dehydration
	2	414.42–468.85	435.39	64.10±1.38	406.35±8.78	22.32	31.51	1.15±0.02	decomposition
	3	500.00–598.09	559.55	43.60±0.94	333.92±7.21	79.60	95.60	1.05±0.02	decomposition
	4	649.56–655.95	651.26	1201.37±25.95	9249.09±199.80	6.27	6.78	2.07±0.04	decomposition
SOL [b]	1	96.13–199.30	149.65	23.48±0.50	98.90±2.13	278.05	657.87	1.19±0.02	dehydration
	2	158.83–171.19	164.19	250.53±5.41	920.82±19.89	3.10	7.09	1.56±0.03	decomposition
	3	407.30–452.00	422.60	68.26±1.47	422.67±9.13	27.80	39.97	1.10±0.02	decomposition
	4	479.18–502.32	480.54	27.46±0.59	198.85±4.29	3.31	4.40	0.70±0.01	decomposition
	5	506.11–593.09	551.00	40.42±0.87	310.48±6.70	73.59	89.31	1.05±0.02	decomposition

[a] Weight of sample taken=6.70 mg; weight of sample after DSC=3.10 mg.
[b] Weight of sample taken=6.53 mg; weight of sample after DSC=3.51 mg.

bands at 605(w), 705(w) and 860(w), give credence [24] to the presence of Na_2CO_3. Moreover, the XRD data (Table 4) confirmed the presence of both, sodium carbonate [22] and lanthanum oxycarbonate [28]. A few additional peaks are present in the XRD which indicate the presence of trace La_2C_3. Prior to the formation of a mixture of carbonates in the TG curve at ca. 538°C, an inflection at 513°C and a small exotherm at 510°C in DTA may be due to the formation of an intermediate, $La_2(CO_3)_3$, which immedi-

ately decomposes to oxycarbonate. Additional peaks in XRD may be due to undecomposed lanthanum carbonate. A change in DTG between 430° and 548°C can be seen from these changes. Similar values of E^* are calculated for this first decomposition step using different non-mechanistic equations [17–20] (Table 2). The DTA profile involves a rapid conversion of an exothermic change at 420°C to an endotherm at 428°C and, subsequently, to an exotherm around 445°C. These are attributed to the partial decomposition of oxalate group with the evolution of CO(g) which, in turn, gets exothermically converted to CO_2(g) at 420°C; the separation of sodium oxalate from $Na[La(C_2O_4)_x]$ and their rearrangement takes place endothermically at 428°C and their subsequent decomposition takes place exothermically in accordance at 445°C. Similar rapid conversions are also reported [29] in the thermal decomposition of $M_3[Fe(CH_2C_2O_4)_3]_2{\cdot}xH_2O$ (where, M=Sr and Ba). Both, Na_2CO_3 and $La_2O(CO_3)_2$ formed at 538°C in TG are stable up to 763°C and beyond this continuous mass loss observed up to 1000°C. The 50% mass loss at ca. 835°C indicates that the carbonate decomposes to an oxide, along with a trace of undecomposed Na_2CO_3. Finally, at 1000°C, the mass loss of 53.5% suggests the formation of Na_2O and $1/2La_2O_3$ contaminated by undecomposed $1/2Na_2CO_3$. IR bands at 415(b), 605(w), 640(w), 705(w) and 860(w) cm^{-1} of the residue isolated after independent pyrolysis in air up to 950°C give evidence [24] of the presence of Na_2CO_3 and La_2O_3. The XRD data (Table 4) confirms [22] the existence of Na_2CO_3, Na_2O, Na_2O_2 and La_2O_3 in the mixture residue. Some more *d*-values are noticed, which may be due to $NaLaO_x$ (where $x<1$ or any integral value from one to three) formed from the solid–solid reaction of the traces of oxides of sodium and lanthanum at high temperatures. The E^* values (Table 2), calculated from the TG curve (763–876°C), are found to be very low as compared to the other steps. The DSC profile (Fig. 4) in nitrogen reveals a large endothermic peak between 96.13° and 199.3°C with a shoulder in the 158.83–171.19°C range, indicating the partial decomposition of the $C_2O_4^{2-}$ group during deaquation. The high E^* (Table 5) value for the shoulder indicates that the partial decomposition takes place very slowly. Further decomposition corresponds to a medium endotherm between 407.3° and 452°C. This is followed by a small hump at 480.54°C (between 479.18° and 502.32°C) corresponding to the formation of an intermediate product which subsequently proceeds to further endothermic decomposition between 506.11° and 593.09°C. The mass loss of 46.25% at 630°C indicates the formation of a mixture of Na_2CO_3, NaO_2 and $1/2La_2O_3$ (calculated mass loss, 47.43%). The IR bands at 640(w), 705(w), 720(S), 858(w) cm^{-1} of the residue confirmed [24] the presence of sodium carbonate and oxide of lanthanum. The kinetic parameters after integration of all the peaks are shown in Table 5.

The foregoing results suggests the following tentative decomposition scheme in air:

$$Na_3[La(C_2O_4)_3]\cdot 8H_2O \overset{\text{ca. } 94^\circ C}{\rightarrow} Na_3[La(C_2O_4)_3]$$

$$\cdot 7H_2O(s) + H_2O(v) \overset{\text{ca. } 230^\circ C}{\rightarrow} Na_3[La(C_2O_4)_3](s)$$

$$+ 7H_2O(v) \overset{\text{ca. } 437^\circ C}{\rightarrow} Na_2C_2O_4(s) + Na[La(C_2O_4)_x](s)$$

$$\overset{\text{ca. } 538^\circ C}{\rightarrow} Na_2CO_3(s) + 1/2La_2O(CO_3)_2(s)$$

$$+La_2C_3(\text{trace}) + xCO(g) + yCO_2(g) \overset{1000^\circ C}{\rightarrow} Na_2O(s)$$

$$+Na_2O_2(s)(\text{trace}) + 1/2Na_2CO_3(s) + 1/2La_2O_3(s)$$

$$+NaLaO_x(s)(\text{trace}) + mCO(g) + nCO_2(g)$$

4. Conclusion

On the basis of thermal studies (TG, DTA and DTG) in air, it is established that the separation of alkali metal oxalate from $Li[La(C_2O_4)_x]$ (where $x=2$ for LOL and $1.5<x<2$ for SOL) takes place during decomposition at about the same temperature in both the complexes. Subsequently, the decomposition of alkali metal oxalate to carbonate is observed in both cases, but La_2O_3 is generated directly from $Li[La(C_2O_4)_2]$ in case of LOL, whereas it is formed in case of SOL through the formation of $La_2O(CO_3)_2$. The lanthanites $LiLaO_2$ and $NaLaO_x$ are produced in case of LOL andSOL, respectively, through the solid–solid reaction of carbonate and/or oxide of alkali metal and La_2O_3. Moreover, the oxide and peroxide of alkali metal and carbides of lanthanum are detected in the decomposition product of both the complexes. The E^* values determined using four non-mechanistic equations are in good agreement with each other for the dehydration and decomposition steps of LOL and SOL.

References

[1] B. Viswanathan, V.R.K. Murthy, Ferrite Materials, Springer-Verlag, Berlin, 1990, p. 86.
[2] N. Tanaka, M. Manjo, Bull. Chem. Soc. Jpn. 40 (1967) 230.
[3] N. Tanaka, K. Sato, Bull. Chem. Soc. Jpn. 43 (1970) 789.
[4] G.M. Bancroft, K.G. Dharmawardena, A.G. Maddock, Inorg. Nucl. Chem. Lett. 6 (1970) 403.
[5] A.S. Brar, B.S. Randhawa, Bull. Chem. Soc. Jpn. 54 (1981) 3166.
[6] B.S. Randhawa, Randhir Singh, Thermochim. Acta 243 (1994) 101.
[7] B.S. Randhawa, P.S. Bassi, Sandeep Kaur, Indian J. Chem., A 28 (1989) 463.
[8] A.S. Brar, B.S. Randhawa, J. Sol. Stat. Chem. 58 (1985) 153.
[9] K. Nagase, Bull. Chem. Soc. Jpn. 46 (1973) 144.
[10] W.W. Wendlandt, E.L. Simmons, J. Inorg. Nucl. Chem. 27 (1965) 2317.
[11] E.L. Simmons, W.W. Wendlandt, J. Inorg. Nucl. Chem. 27 (1965) 2325.
[12] N. Deb, S.D. Baruah, N.N. Dass, J. Therm. Anal. 45 (1995) 457.
[13] N. Deb, S.D. Baruah, N.N. Dass, Thermochim. Acta 285 (1996) 301.
[14] T.K. Sanyal, N.N. Dass, J. Inorg. Nucl. Chem. 42 (1980) 811.
[15] N. Deb, P.K. Gogoi, N.N. Dass, Bull. Chem. Soc. Jpn. 61 (1988) 4485.
[16] K. Nakamoto, Infrared Spectra of Inorganic and Coordination Compounds, second edn., Wiley–Interscience, New York, 1969, pp. 83, 89, 219, 245.
[17] E.S. Freeman, B. Carroll, J. Phys. Chem. 62 (1958) 394.
[18] J.H. Flynn, L.A. Wall, J. Res. Nat. Bur. Stand., Sect. A. 70 (1966) 6.
[19] A.W. Coats, J.P. Redfern, Nature 201 (1964) 68.
[20] J.R. MacCallum, J. Tanner, Eur. Polym. J. 6 (1970) 1033.
[21] K.V. Krishnamurty, G.M. Harris, Chem. Rev. 61 (1961) 213.
[22] Joint Committee on Powder Diffraction Standards, Inorganic Index to the Powder Diffraction File, 1971, 1601, Parklane, PA.
[23] R.A. Nyquist, R.O. Kagel, Infrared Spectra of Inorganic Compounds, Academic Press, New York, 1971.
[24] F.F. Bentley, L.D. Smithson, A.L. Rozek, Infrared Spectra and Characteristic Frequencies, 300–700 cm^{-1}, Wiley–Interscience, New York, 1968.
[25] J.A. Dean, Lange's Handbook of Chemistry, thirteenth edn., MacGraw–Hill, New York, 1987, pp. 4–69.
[26] B.S. Randhawa, P.S. Bassi, Sandeep Kaur, J. Radioanal. Nucl. Chem. Lett. 188(4) (1994) 279.
[27] B.S. Randhawa, J. Radioanal. Nucl. Chem. Lett. 201(1) (1995) 57.
[28] S.R. Dharwadkar, M.S. Kumbhar, M.S. Chandrasekharaiah, M.D. Kharkhanavala, J. Inorg. Nucl. Chem. 42 (1980) 1621.
[29] P.S. Bassi, B.S. Randhawa, Sandeep Kaur, Indian J. Chem., A 31 (1992) 596.